EXPERIMENTAL MODELLING OF IR NONLINEAR PHOTOTHERMAL RADIOMETRY IN CARBON/EPOXY COMPOSITE MATERIALS

G.Kalogiannakis[1], S. Longuemart[2], J. Ravi[2], D. Van Hemelrijck[1] and C. Glorieux[2]
[1] Vrije Universiteit Brussel, Dept of Mechanics of Materials and Constructions, Brussels, Belgium; [2]Laboratorium voor Akoestiek en Thermische Fysica (ATF), Department of Physics and Astronomy, K.U.Leuven, Belgium

Abstract: The potential of thermal nonlinear effects in composite materials was investigated for non-destructive testing. Second harmonic generation in thermal-wave fields has attracted much attention in recent years for the non-destructive evaluation of solid structures. Even though not the only source, the presence of a defect can result in a strong nonlinear signature, which could enhance the detectability of photothermal methods. The following experimental survey trails several theoretical analyses on the subject, mostly for homogeneous isotropic samples. As composite material structures exhibit often thermo-mechanical nonlinearities originating from the polymer matrix, they appeared to be ideal candidates to exploit the potential of nonlinear photothermal radiometry. In this work, a theoretical model that was recently developed is used to estimate the generated overtones that originate from the most common cause of failure of composites, the delamination. Moreover, the theory is experimentally validated using IR photothermal radiometry by modelling the oscillation of the size of the delamination by means of a piezoelectric transducer.

Introduction: In principle, nonlinear photothermal radiometry exploits higher harmonic signal generation for non-destructive testing. The temperature field imposed by amplitude modulated laser excitation depends on variations in thermal properties [1-3] as well as the synchronous modification of the boundary conditions [4, 5]. Such effects, which are closely linked with the present of a defect, allow enhancing the contrast of a defected area by detecting the second harmonic temperature signal.

The theoretical potential of using nonlinear photothermal radiometry in fibre reinforced composite materials partially emerged as measurements demonstrated recently that the thermal properties exhibit strong dependence on temperature [2, 3]. Nonlinear effects are often present in composites, and originate from the thermomechanical behaviour of the polymer matrix. Numerical analysis using a finite element model of this particular nonlinearity has motivated to perform an experimental examination. When a defect is introduced in an intact sample, spectral analysis shows that the second harmonic of the surface temperature signal is affected much more than the fundamental frequency component. Although the contrast for both signal components follows the same pattern for the fundamental and the second harmonic, the respective relative values are strongly different. This implies in practice a better visibility of the defect.

Moreover, delaminations are very often formed in composites due to large interlaminar shear stresses. Modulated laser excitation alters the uniform temperature field to a gradient with higher temperatures near the surface. Therefore, non-uniform thermal expansion results in thermoelastic bending, the modulation of which imposes a vibration of the layer above the delamination [6] at the excitation frequency. The triggered oscillation of the air gap in the delamination entails an alteration of the boundary condition for the heat diffusion problem. This phenomenon was first accredited to explain the strong nonlinearities observed [7]. Later it was shown theoretically that this effect can be really effective [4].

In this work, a theoretical model that was recently developed [12] is validated experimentally. The model was used to estimate the influence of the oscillation of the size of a defect on the photothermal signal and the order of magnitude of the second harmonic that is generated under conditions. To this end, a composite sample was tested in combination with a metallic substrate that was enabled to vibrate independently.

Theoretical background: The thermal and the displacement-wave fields in a solid are in general coupled through the equations of thermoelastodynamics [8]. These equations are formulated for a homogeneous anisotropic unbounded medium as follows:

$$C_{ijkl}u_{k,lj} + f_i = \rho\ddot{u}_i$$
$$f_i = -\beta_{ij}\theta_{ij} \quad (1)$$
$$\rho C_p\dot{\theta} - k_{ij}\theta_{,ij} + T_0\beta_{ij}\dot{u}_{i,j} = Q$$

where Einstein's convention on the indices i, j, k and l is adopted. The displacement field $\boldsymbol{u}$ is a vector-valued function, while the change of temperature θ with respect to a given initial temperature distribution, is a scalar-valued function. In the wave equation, the components of the fourth order tensor $\boldsymbol{C}$ represent the adiabatic elastic constants, ρ is the density and the vector-valued function $\boldsymbol{f}$ consists of the body forces. These forces depend linearly on the temperature field by means of the tensor $\boldsymbol{\beta}$, the components of which depend on the thermal coefficients of linear expansion $\boldsymbol{\alpha}$, as shown in the following equation:

$$\beta_{ij} = C_{ijkl}\alpha_{kl} \quad (2)$$

In the heat diffusion equation, C_p is the specific heat per unit volume at constant pressure and $\boldsymbol{k}$ is the conductivity tensor. In what follows, according to the theory of thermal stresses, the source term $T_0\beta_{ij}\dot{u}_{i,j}$ of thermoelastic origin on the left-hand side has minor contribution and so can be neglected.

The solution for the strongly damped thermal-wave field introduces a gradient of temperature and consequently a gradient of thermal expansion (thermoelastic bending) that enables the vibration of a thin plate above a delamination at the excitation frequency (fig. 1). To attain thermoelastic bending the thickness of the plate should be much smaller than its lateral dimensions. Effects of thermoelastic bending overshadowing the thermal dilatation have been reported before by several scientists [6, 7].

Provided that there is vibration it is straightforward to show that the temperature at the surface can be approximated by a mixture of the two components of the extremes. Consider, for instance, a delamination with an initial air gap thickness d_0 that oscillates independently at frequency ω_1. If the amplitude of the oscillation is ε, then the air gap thickness at any time t is given by:

$$d=d_0 + \varepsilon\sin(\omega_1 t) \quad (3)$$

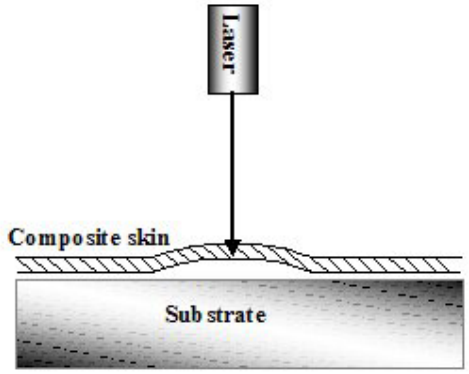

Fig. 1. Thermoelastic bending.

The amplitude A and the phase ϕ of the thermal wave at the surface are functions of the excitation frequency ω_2 as well as the thickness of the delamination air gap d. It has been mathematically shown [12] that using the fact that □/d_0 is very small and expanding in Taylor series disregarding higher orders A and φ can be expressed as follows:

$$T(t) = A(\omega_2, \mathrm{d}_0 + \varepsilon \sin(\omega_1 t)) \sin(\omega_2 t + \phi(\omega_2, \mathrm{d}_0 + \varepsilon \sin(\omega_1 t)))$$
$$= \left(A(\mathrm{d}_0) + \frac{\partial A}{\partial d} \varepsilon \sin(\omega_1 t) \right) \sin\left(\omega_2 t + \phi(\mathrm{d}_0) + \frac{\partial \phi}{\partial d} \varepsilon \sin(\omega_1 t) \right) \quad (4)$$

In the terms oscillating at frequency ω_1, the factors $\frac{\partial A}{\partial d}\varepsilon$ and $\frac{\partial \phi}{\partial d}\varepsilon$ can be expressed as follows:

$$\frac{\partial A}{\partial d}\varepsilon = \frac{A(d_0 + \varepsilon/2) - A(d_0 - \varepsilon/2)}{\varepsilon}\varepsilon = A(d_0 + \varepsilon/2) - A(d_0 - \varepsilon/2)$$
$$\frac{\partial \phi}{\partial d}\varepsilon = \frac{\phi(d_0 + \varepsilon/2) - \phi(d_0 - \varepsilon/2)}{\varepsilon}\varepsilon = \phi(d_0 + \varepsilon/2) - \phi(d_0 - \varepsilon/2) \quad (5)$$

For the case where the thickness oscillations are induced by the probing thermal wave field itself, ω_1 and ω_2 *are equal*, and the temperature signal exhibits oscillation at both frequencies ω and 2ω. The amplitude and phase of the second harmonic are provided by the difference in the characteristic values for the two extremes of the vibration.

Experimental setup: The experimental setup, shown in Figure 2, consists of a diode pumped solid-state laser (DPSS, Λ=532 nm) intensity modulated by an acousto-optic modulator (IntraAction), a lens, the position of which controls the spot size of the laser beam, the computer controlled 3D stage for supporting and positioning the sample, and an infrared detector. A germanium window with a transmission bandwidth of 2-14 μm is mounted in front of the detector to block any visible radiation from the pump laser. The infrared emission from the sample is collected and focused to a liquid N_2 cooled HgCdTe (MCT) detector (bandwidth 2-12 microns and sensing area 0.05 x 0.05 mm) using two 90-degree offaxis gold-coated paraboloidal mirrors. The signal from the detector is amplified and fed to a lock-in-amplifier (SR 830). The sample is positioned on the horizontal plane on a three-dimensional translation stage in order to allow adjusting the distance at the focus of the parabolic mirror as well as performing the area scans.

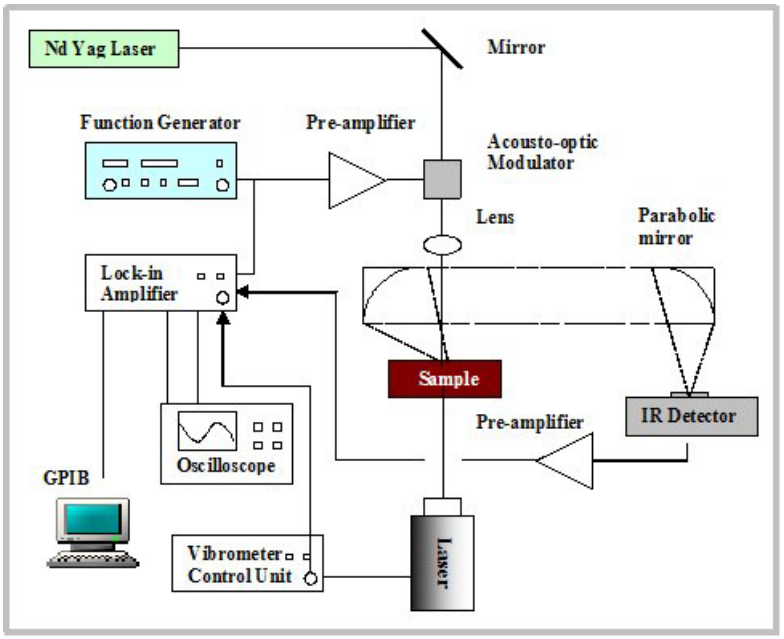

Fig. 2. Experimental setup for IR photothermal radiometry.

In order to perform the measurements, two samples were manufactured, which are depicted in figure 3. A cross-ply laminate was prepared consisting of carbon fibre reinforced epoxy resin (prepreg fibredux 920). A hole (diameter 6mm) was opened with the milling machine reducing the thickness to a thin layer of 180μm. Then a mushroom-like aluminium piece was made to fit exactly inside the hole. The combination of the two pieces enabled to control the air gap in between the thin composite layer and the metallic substrate (fig 3). To this end, the aluminium piece was glued to a piezoelectric transducer which was used to vibrate the substrate at a specific frequency. In order to know the exact displacement a laser vibrometer was used to measure the displacement at different frequencies.

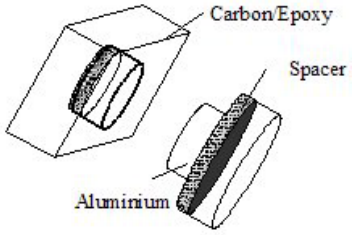

Fig. 3. Carbon/Epoxy sample and matching mushroom-like aluminium piece.

Results: In order to measure the displacement of the vibrating aluminium piece, the Laser vibrometer method was used. The velocity output was fed to a lock-in amplifier and the displacement was then calculated from:

$$\varepsilon = \frac{V}{2\pi f} \tag{6}$$

where V is the velocity amplitude and f is the frequency of the oscillation. The results for a frequency range from 0.1Hz to 100Hz are presented in figure 4.

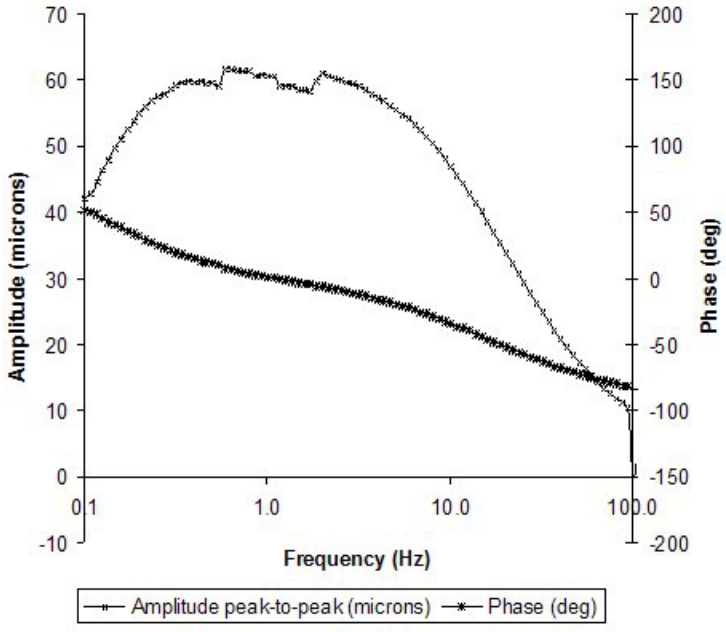

Fig. 4. Measurement of the vibration amplitude and phase of the surface of the aluminium piece connected to a piezoelectric transducer with the Laser vibrometer method.

In the sequence the metallic piece was placed in the Carbon/Epoxy sample and the set was examined with the photothermal radiometry setup. Each of the pieces was positioned on a different translation stage in order to allow controlling the air gap between each other. For better accuracy, the initial air gap was determined by fitting the photothermal signal at the surface using a one-dimensional analytical model. This fitting is depicted in figure 5 and the corresponding values of the thermal properties and the geometrical characteristics are given in Table 1.

Table 1. Thermal properties and geometrical characteristics.

Fitting parameters	Carbon/Epoxy	Air	Aluminium
Thermal Diffusivity (m^2/sec)	$4.56e^{-7}$	$1.99e^{-5}$	$9.72e^{-5}$
Thermal Conductivity (W/m.K)	0.722	0.0258	237
Thickness (μm)	185	64.5	5000

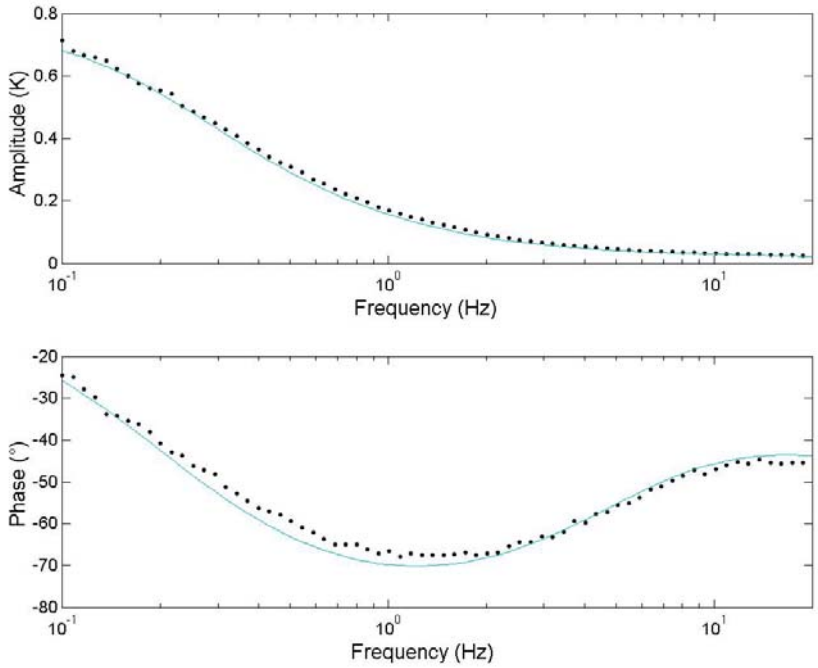

Fig. 5. Fitting of the photothermal signal at the surface of the Carbon/Epoxy sample.

Therefore, switching on the piezoelectric transducer results in a periodic oscillation of the air gap with very well known conditions. To investigate the effect of this oscillation to the photothermal signal, as it was predicted in the relevant theory, the aluminium piece was subjected to vibration at 0.1Hz. The signal of the IR detector was locked at the optimized frequency of 1Hz setting the time constant at 1 second so as to avoid averaging of the low frequency signal. The analog output of each channel (amplitude and phase) of the lock-in amplifier was then fed to an oscilloscope where it was recorded for adequately large time duration (1000 seconds or 100 periods of the low frequency) so as to enable the application of a Fast Fourier Transform. In the following figures, the power spectra are drawn for the signal of the lock-in amplifier. In the first figure (fig.6), the spectra correspond to the case of the

piezoelectric transducer switched off. It is clear that there is only low frequency noise due to the short time constant.

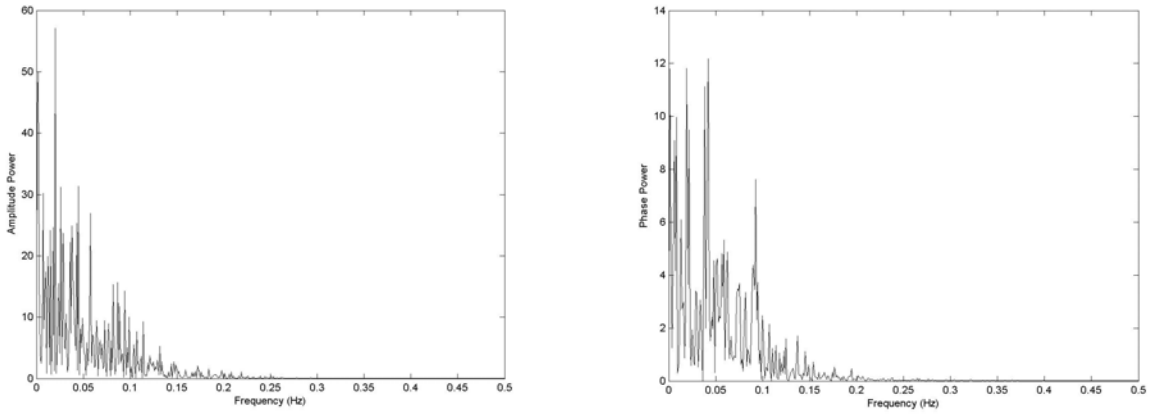

(a) (b)

Fig. 6. The power spectra of the photothermal signal for the piezoelectric transducer switched off. (a) amplitude power spectrum and (b) phase power spectrum.

In figure 7, though, the peak clearly designates the component at the low frequency of the vibration as it was predicted by eq. (4).

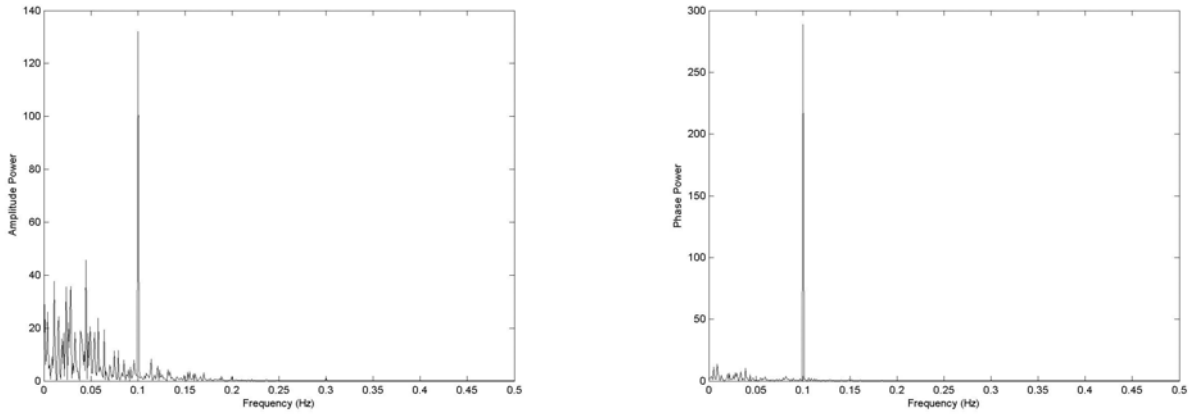

(a) (b)

Fig. 7. The power spectra of the photothermal signal for the piezoelectric transducer switched on. (b) amplitude power spectrum and (b) phase power spectrum.

A simulation of the photothermal signal based on a one-dimensional model for static cases and the theory in the first section gives an indication about the validity of the results and vice-versa. The results are drawn in figure 8. The phase and amplitude differences at 1 Hz fit very well with the respective strength of the power spectra.

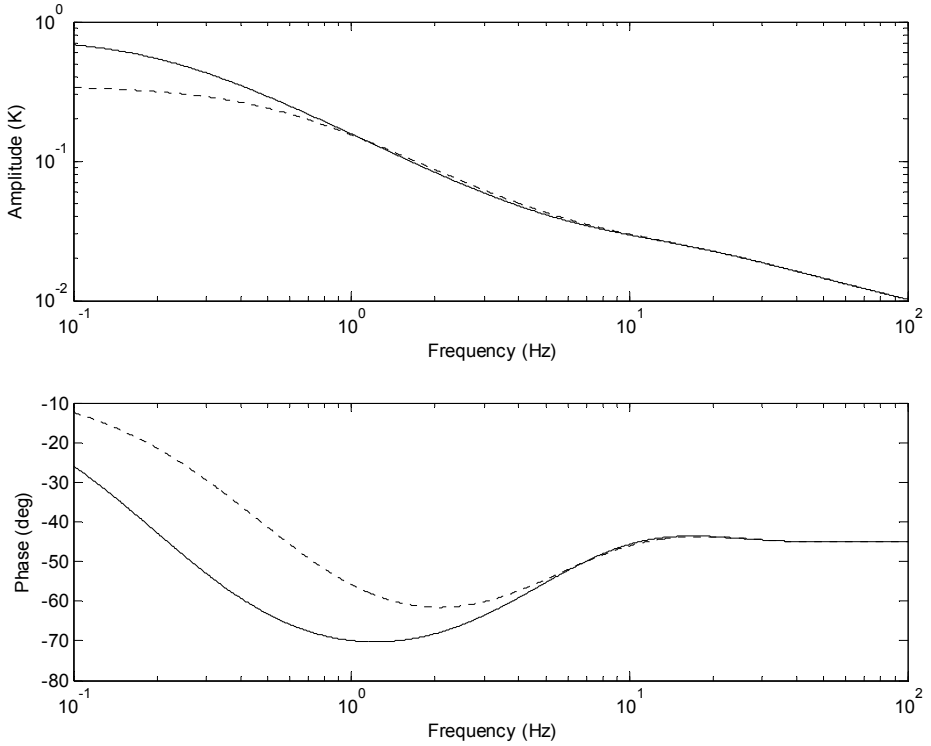

Fig. 8. Simulation of the photothermal signal for static air gaps of 65μm (dotted line) and 25μm (solid line).

Finally, the existence of a second harmonic component was examined using identical frequencies for the vibration of the transducer and the excitation. At this point it should be stressed that there are intrinsic overtones in the method from various sources. One of these sources is the inefficiency in providing a pure sine excitation and the other is associated with the nonlinear detector response originating from the Stefan-Boltzmann law. The former one is resolved by applying a square function excitation but the latter is rather inevitable. Unfortunately, due to the difference in the displacement response of the piezoelectric transducer with respect to the frequency it was not possible to run a frequency scan. Instead, it was just examined for this single frequency of 1Hz. The results are given in Table 2. It is readily observed that the second harmonic is strongly affected by the oscillation of the air gap.

Table 2. The influence of the air gap oscillation on the second harmonic photothermal signal.

Status of the piezoelectric transducer	Amplitude		Phase	
	f	*2f*	*f*	*2f*
ON	3.78mV	178μV	-104.88°	64.5°
OFF	3.29mV	46.2μV	-103.38°	109.3°

Conclusions: Experimental modelling was used to demonstrate the nonlinearities that arise from the existence of a defect during the detection with photothermal techniques and how these can enhance the contrast of a defect. The theory that was recently used to estimate the magnitude of the second harmonic component in the signal as a result of the oscillation of the defect thickness was validated. The oscillation of the air gap of the delamination could be detected both at a different frequency and at the second harmonic of the excitation frequency.

References:

[1] Gusev, V., Mandelis, A. & Bleiss R, 1992. "Theory of Second Harmonic Thermal-Wave Generation: One-Dimensional Geometry", *Int. J. Therm.* 14/2 , 321-337.

[2] Kalogiannakis G., Van Hemelrijck D. & Van Assche G, 2004. "Measurements of thermal properties of Carbon/Epoxy and Glass/Epoxy using Modulated Temperature Differential Scanning Calorimetry", J.Comp. Mater. **38**/2, p. 163-175.

[3] Kalogiannakis, G., Van Hemelrijck, D, 2003. "Contrast enhancement of Nonlinear Photothermal Radiometry in composite materials". *Proc. 3rd Int. Conf. on Emerging Technologies in NDT,* Thessaloniki, 26-28 May 2003.

[4] Gusev, V., Mandelis, A. & Bleiss R, 1992. "Theory of Strong Photothermal Nonlinearity from Sub-Surface Non-Stationary ("Breathing") Cracks in Solids". *J. Appl. Phys.* **A57**: 229-233.

[5] Mandelis, A., Salnick, A., Opsal, J. & Rosencwaig, A, 1999. "Nonlinear fundamental thermal response in three-dimensional geometry: Theoretical model", *J. Appl. Phys.* **85**/3, 1811-1821.

[6] Cielo, P., Maldague, X., Rousset, G. & Jen, CK, 1985. "Thermoelastic inspection of layered materials: dynamic analysis". *Mater. Eval.* **43**/9, 1111-1116.

[7] Rajakarunanayake, Y.N. & Wickramasinghe, H.K, 1986. *Appl. Phys. Lett.* **48,** 218

[8] Nowacki W, 1986. "Thermoelasticity", Pergamon Press, ISBN 0-08-024767-9

[9] Almond D., Patel P., 1996. "Photothermal Science and Techniques", Chapman and Hall, London

[10] Roark R.J. & Young W.C. "Formulas for Stress and Strain", Mc Graw Hill Book Company, ISBN 0-07-053031-9

[11] Lauriks W., Desmet C., Glorieux C. & Thoen J, 1993. "Investigation of the thermal anisotropy of unidirectional carbon fiber reinforced composite plates using optically generated thermal waves and a noncontact optical detection technique" *J. Mater. Res.* **8**/12

[12] Kalogiannakis G., Ravi J., Longuemart S., Bentefour E. H., Van Hemelrijck D. and Glorieux C., 2004. "IR nonlinear photothermal radiometry in Carbon/Epoxy composite materials: Experimental survey", Proc. Of 11th European Conference on composite materials, Rhodes 31 May – 3rd June 2004, Greece